MSW mediated neutrino decay and the solar neutrino problem

Abhijit Bandyopadhyay,* Sandhya Choubey,† and Srubabati Goswami‡
Saha Institute of Nuclear Physics, 1/AF, Bidhannagar, Calcutta 700 064, India
(Received 25 January 2001; published 10 May 2001)

We investigate the solar neutrino problem assuming the simultaneous presence of MSW transitions in the Sun and neutrino decay on the way from the Sun to Earth. We do a global χ^2 analysis of the data on the total rates in Cl, Ga, and SuperKamiokande (SK) experiments and the SK day-night spectrum data and determine the changes in the allowed region in the Δm^2 -tan$^2\,\theta$ plane in the presence of decay. We also discuss the implications for unstable neutrinos in the SNO experiment.

DOI: 10.1103/PhysRevD.63.113019 PACS number(s): 14.60.Pq, 13.35.Hb, 26.65.+t, 96.40.Tv

I. INTRODUCTION

Global analysis of the total rates measured in the Cl, Ga [1], and SuperKamiokande (SK) experiments and the day-night spectrum data of SK [2] indicate that the large mixing angle (LMA) Mikheyev-Smirnov-Wolfenstein (MSW) solution gives the best description of the solar neutrino data [3]. However, before a particular solution can be established one should rule out other possibilities. In this spirit physicists have considered various nonstandard neutrino properties and their implications for the solar neutrino problem [4]. In this paper we consider a scenario where neutrinos are allowed to decay on their way from the Sun to Earth after undergoing MSW transitions in the Sun. Such a possibility was discussed earlier in [5].

We consider two-flavor mixing between ν_e and ν_μ/ν_τ with mass eigenstates ν_1 and ν_2. We assume that the heavier mass state ν_2 is unstable, while the lighter neutrino mass state ν_1 has a lifetime much greater than the Sun-Earth transit time and hence can be taken as stable. There are two possible nonradiative decay modes.[1]

Model 1: If neutrinos are Dirac particles, one has the decay channel $\nu_2 \to \overline{\nu}_{1R} + \phi$, where $\overline{\nu}_{1R}$ is a right handed singlet and ϕ is an isosinglet scaler. Thus all the final state particles for this model are sterile and there is no distinct signature of this decay apart from disappearance experiments. This model is discussed in [7]. In this model a light scalar boson ϕ with lepton number -2 and a singlet right handed neutrino is added to the standard model. The neutrino coupling to this scalar boson is given by $g_{21}\nu_{R_1}^T C^{-1}\nu_{R_2}$, C being the charge conjugation operator.

Model 2: If neutrinos are Majorana particles, the decay mode is $\nu_2 \to \overline{\nu}_1 + J$, where J is a Majoron, produced as a result of spontaneous breaking of a global $U(1)_{L_e - L_\mu}$ symmetry [8]. In this model the neutrino masses are generated by extending the Higgs sector of the standard model. Though the original triplet Majoron model proposed by Gelmini and Roncadeli [9] is ruled out from the CERN e^+e^- collider LEP data on Z decay to invisible modes [10], the model discussed in [8], which needs two additional triplet bosons and one singlet scalar boson in the theory, can avoid conflict with the LEP data and at the same time predict a fast enough neutrino decay necessary to solve the solar neutrino problem. In this model the $\overline{\nu}_1$ can be observed as a $\overline{\nu}_e$ with a probability $|U_{e1}|^2$ and as a $\overline{\nu}_\mu/\overline{\nu}_\tau$ with a probability $|U_{e2}|^2$.

In both the decay scenarios the rest frame lifetime of ν_2 is given by [11]

$$\tau_0 = \frac{16\pi}{g^2}\,\frac{m_2(1+m_1/m_2)^{-2}}{\Delta m^2}, \tag{1}$$

where g is the coupling constant, m_i is the ν_i mass, and $\Delta m^2 = m_2^2 - m_1^2$. Assuming $m_2 \gg m_1$ Eq. (1) can be written as

$$g^2 \Delta m^2 \sim 16\pi\alpha, \tag{2}$$

where α is the decay constant related to τ_0 as $\alpha = m_2/\tau_0$. If we now incorporate the bound $g^2 < 4.5\times10^{-5}$ as obtained from K decay modes [12], we get the bound[2] $\Delta m^2 > 10^6\alpha$. Since for a typical neutrino energy of 10 MeV, one starts getting decay effects over the Sun-Earth distance for $\alpha \gtrsim 10^{-13}$ eV^2, the corresponding limit on Δm^2 is $\Delta m^2 \gtrsim 10^{-7}$ eV^2. In an earlier paper we considered high values of Δm^2 ($>10^{-3}$ eV^2) so that matter effects inside the Sun can be neglected and one can have decay as well as Δm^2 independent average oscillations [14]. In this paper we consider $10^{-6} \leqslant \Delta m^2 \leqslant 10^{-3}$ eV^2 such that matter effects inside the Sun are important. We incorporate Earth matter effects as well.

In Sec. II we discuss the usual two-flavor MSW solutions to the solar neutrino problem. We perform a χ^2 analysis to the global data on rates and SK day-night spectrum and present the allowed regions in the Δm^2-tan$^2\,\theta$ plane. In Sec. III we introduce the possibility of having one of the neutrino states ν_2 as unstable. We look for the effects of decay on the MSW solutions and present the allowed areas at

*Email address: abanerjee@tnp.saha.ernet.in
†Email address: sandhya@tnp.saha.ernet.in
‡Email address: sruba@tnp.saha.ernet.in

[1]Radiative decays are severely constrained [6].

[2]Since the m_{ee} element of the mass matrix is zero in the Majoron decay model considered, the 0ν Majoron $\beta\beta$ decay does not take place in this model [8] and the more stringent bound on g from Majoron emission in $\beta\beta$ decay [13] is not applicable.

TABLE I. The best-fit values of the parameters, χ^2_{min} and the goodness of fit from the global analysis of the rates and day-night spectrum data for the MSW analysis involving two neutrino flavors.

	Nature of solution	Δm^2 in eV^2	$\tan^2\theta$	χ^2_{min}	Goodness of fit
	SMA	5.48×10^{-6}	5.79×10^{-4}	43.22	19.01%
X_B fixed	LMA	4.17×10^{-5}	0.35	37.33	40.78%
at SSM value	LOW	1.51×10^{-7}	0.64	39.54	31.48%
	SMA	5.35×10^{-6}	4.34×10^{-4}	37.98	33.51%
X_B varying	LMA	4.22×10^{-5}	0.25	34.20	50.67%
	LOW	1.51×10^{-7}	0.64	39.88	26.20%

various values of the decay constant. We show that for the Majoron decay model (model 2) the SK data on $\overline{\nu}_e$-p events restricts the allowed values of the decay constant to extremely low values. In Sec. IV we discuss the implications of nonzero neutrino decay for the SNO experiment. We finally present our conclusions in Sec. V.

II. MSW EFFECT FOR STABLE NEUTRINOS

As was first indicated in [15], the interaction of electron neutrinos propagating through the Sun modifies the vacuum mixing angle θ to the matter mixing angle θ_M where

$$\tan 2\theta_M = \frac{\Delta m^2 \sin 2\theta}{\Delta m^2 \cos 2\theta - 2\sqrt{2} G_F n_e E}. \tag{3}$$

Here n_e is the ambient electron density, E the neutrino energy, and Δm^2 $(=m_2^2-m_1^2)$ the mass squared difference in vacuum. The vanishing of the denominator in Eq. (3) defines the resonance condition, where the matter mixing angle is maximal.

The probability amplitude of survival for an electron neutrino is given by

$$A_{ee} = A^{\odot}_{e1} A^{vac}_{11} A^{\oplus}_{1e} + A^{\odot}_{e2} A^{vac}_{22} A^{\oplus}_{2e}, \tag{4}$$

where $A^{\odot}_{ek}$ gives the probability amplitude of a $\nu_e \to \nu_k$ transition at the solar surface,

$$A^{\odot}_{ek} = a^{\odot}_{ek} e^{-i\phi^{\odot}_k}, \tag{5}$$

$$a^{\odot\,2}_{e1} = P_J \sin^2\theta_M + (1-P_J)\cos^2\theta_M = 1 - a^{\odot\,2}_{e2}. \tag{6}$$

Here P_J is the nonadiabatic level jumping probability between the two mass eigenstates for which we use the standard expression from [16]:

$$P_J = \frac{\exp(-\gamma \sin^2\theta) - \exp(-\gamma)}{1-\exp(-\gamma)}, \tag{7}$$

$$\gamma = \pi \frac{\Delta m^2}{E} \left| \frac{d \ln n_e}{dr} \right|^{-1}_{r=r_{res}}. \tag{8}$$

Here A^{vac}_{kk} is the transition amplitude from the solar surface to Earth's surface:

$$A^{vac}_{kk} = e^{-iE_k(L-R_{\odot})}, \tag{9}$$

where L is the Sun-Earth distance and $R_{\odot}$ the radius of the Sun. $A^{\oplus}_{ke}$ denotes the $\nu_k \to \nu_e$ transition amplitudes inside the Earth. We evaluate these amplitudes by assuming the Earth to consist of two constant density slabs. The ν_e survival probability is given by

$$\begin{aligned} P_{ee} &= |A_{ee}|^2 \\ &= a^{\odot\,2}_{e1} |A^{\oplus}_{1e}|^2 + a^{\odot\,2}_{e2} |A^{\oplus}_{2e}|^2 \\ &\quad + 2 a^{\odot}_{e1} a^{\odot}_{e2} Re[A^{\oplus}_{1e} A^{\oplus}{}^{*}_{2e} e^{i(E_2-E_1)(L-R_{\odot})} e^{i(\phi_{2,\odot}-\phi_{1,\odot})}]. \end{aligned} \tag{10}$$

It can be shown that the square bracketed term containing the phases average out to zero in the range of Δm^2 in which we are interested [17].

Using Eq. (10) as the probability we have done a χ^2 analysis of the current solar neutrino data on total rates from[3] Cl, Ga [1], and SK and the 18+18 bins of data on the day-night electron energy spectrum from SK [18]. The details of the code used can be found in [19]. We use the 1117-day data of SK and incorporate the 2000 Bahcall-Basu-Pinsonneault (BBP00) solar model [20]. The theory errors and their correlations in the analysis of total rates are included as in [21]. In addition to the astrophysical uncertainties included in [19] for the analysis of the total rates, we have included the uncertainty in the S_0 factor for the reaction $^{16}O(p,\gamma)^{17}F$ [20]. For the day-night spectrum analysis we have included the correlation between the systematic errors of the day and the night bins [22]. As in [23] we vary the normalization of the spectrum as a free parameter which avoids the overcounting of the rates and spectrum data for SK. Hence for the day-night spectrum analysis we have 36 -1 degrees of freedom (DOF) while for the total rates we have 3, which makes a total of 38 DOF for the rates +spectrum analysis with no oscillation. For the MSW analysis with two active neutrino flavors we present in Table I two sets of results: (i) with the ^8B normalization factor X_B in the

[3]We use the weighted average of the rates from SAGE, GALLEX, and GNO.

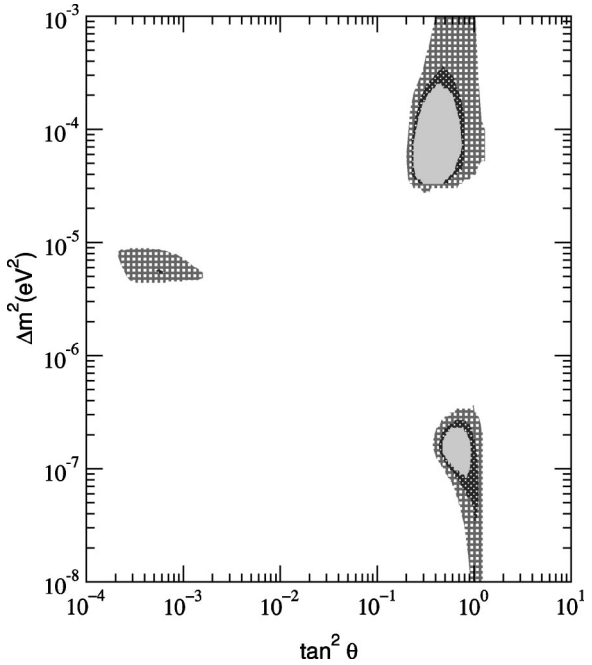

FIG. 1. The 90%, 95%, and 99% C.L. allowed area from the global analysis of the total rates from Cl, Ga, and SK detectors and the 1117-day SK recoil electron spectrum at day and night, assuming MSW conversions to stable sequential neutrinos.

total rates held at the SSM value; (ii) with the ^8B normalization factor X_B in the total rates kept as a free parameter.

The best fit comes in the LMA region. In Fig. 1 we plot the 90%, 95%, and 99% C.L. allowed regions for the two-flavor MSW transition to an active neutrino. All the contours have been drawn with respect to the global minimum with X_B fixed at the SSM value. We have also done a χ^2 analysis for $\nu_e - \nu_s$ MSW conversion, ν_s being a sterile neutrino, for both X_B fixed at SSM and X_B varying freely. The best-fit values of the parameters, χ^2_{min} and the goodness of fit (GOF) are $\Delta m^2 = 3.74\times10^{-6}$ eV^2, $\tan^2\theta = 5.2\times10^{-4}$, $\chi^2_{min} = 44.85$, GOF$= 14.79\%$, X_B fixed at the SSM value and $\Delta m^2 = 3.71\times10^{-6}$ eV^2, $\tan^2\theta = 4.72\times10^{-4}$, $\chi^2_{min} = 43.42$, GOF$= 15.53\%$, X_B free.

III. MSW EFFECT AND UNSTABLE NEUTRINOS

If a neutrino of energy E decays while traversing a distance L, then the decay term $\exp(-\alpha L/E)$ gives the fraction of neutrinos that survive, where α is the decay constant discussed before. In Fig. 2 we plot this $\exp(-\alpha L/E)$ as a function of α for two different energy values. For α very small the exponential term is ≈ 1 and there is no decay. As α increases one starts getting decay over the Sun-Earth distance only for $\alpha \gtrsim 10^{-13}$ eV^2. As we have discussed in the Introduction, since from K decay $\Delta m^2 \geqslant 10^6\alpha$, one can have simultaneous MSW and decay for 10^{-7} eV$^2 < \Delta m^2 < 10^{-3}$ eV^2. Below this Δm^2 the bound on the coupling constant coming from K decay restricts the decay constant α to be small enough so that decay effects are negligible over the Sun-Earth distance. So henceforth we will be concerned with only the LMA and small mixing angle (SMA) solutions,

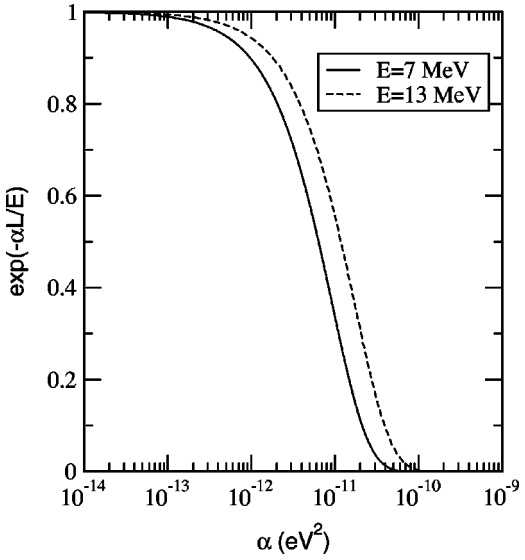

FIG. 2. The decay term $\exp(\alpha L/E)$ vs α for two different neutrino energies. L is taken as the Earth-Sun distance.

the low probability, low mass (LOW) region remaining unaffected due to decay. For $\Delta m^2 > 10^{-3}$ eV^2 there will not be any MSW effect.

The probability amplitude for ν_e survival in the presence of neutrino decay is again given by Eq. (4), with $A^{\odot}_{ek}$, $A^{\oplus}_{ke}$, and A^{vac}_{11} as before, the only change being for A^{vac}_{22} since the ν_2 decays on its way from the Sun to Earth. A^{vac}_{22} is given by

$$A^{vac}_{22} = e^{-iE_2(L-R_\odot)} e^{-\alpha(L-R_\odot)/E_2}. \tag{11}$$

Then, the ν_e survival probability is given by (ignoring the phase part)

$$P_{ee} = a^{\odot\,2}_{e1} |A^{\oplus}_{1e}|^2 + a^{\odot\,2}_{e2} |A^{\oplus}_{2e}|^2 e^{-2\alpha(L-R_\odot)/E_2}. \tag{12}$$

The day-time probability (i.e., without the Earth effect) is given by

$$\begin{aligned} P^{\rm day}_{ee} = {} & \cos^2\theta [P_J \sin^2\theta_M + (1-P_J)\cos^2\theta_M] \\ & + \sin^2\theta [(1-P_J)\sin^2\theta_M + \cos^2\theta_M P_J] \\ & \times e^{-2\alpha(L-R_\odot)/E_2}. \end{aligned} \tag{13}$$

From Eq. (13) we note that the decay term appears with a $\sin^2\theta$ and is therefore appreciable only for large enough θ. Thus we expect the effect of decay to be maximum in the LMA region. This can also be understood as follows. The ν_e are produced mostly as ν_2 in the solar core. In the LMA region the neutrinos move adiabatically through the Sun and emerge as ν_2 which eventually decays. For the SMA region on the other hand P_J is nonzero and ν_e produced as ν_2 cross over to ν_1 at the resonance and come out as a ν_1 from the solar surface. Since ν_1 is stable, decay does not affect this region. Including the Earth effect the survival probability can be expressed as

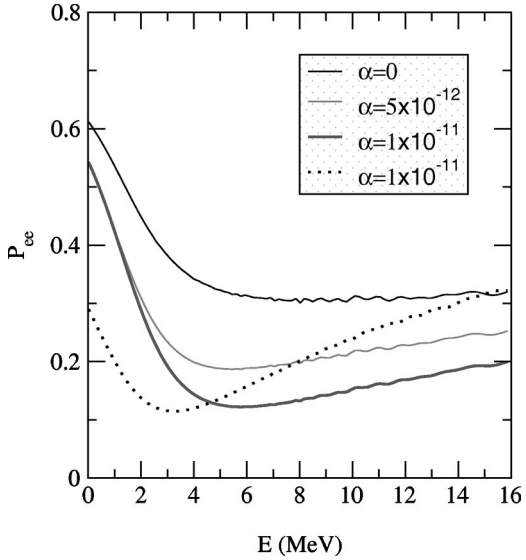

FIG. 3. The survival probability as a function of ν_e energy for different values of α. The solid lines are for $\tan^2\theta=0.35$ while the dotted line is for $\tan^2\theta=0.85$. For all the curves $\Delta m^2=4.17\times10^{-5}$ eV^2.

$$P_{ee}=P_{ee}^{\rm day}+\frac{(\sin^2\theta-P_{2e})[P_{ee}^{\rm day}+e^{-2\alpha(L-R_\odot)/E_2}(P_{ee}^{\rm day}-1)]}{\cos^2\theta-\sin^2\theta e^{-2\alpha(L-R_\odot)/E_2}}. \quad (14)$$

Here P_{2e} is the probability of the second mass eigenstate to get converted into the ν_e state at the detector.

In Fig. 3 the solid lines show the survival probability versus neutrino energy for three different values of α with Δm^2 and $\tan^2\theta$ fixed at the best-fit value of the LMA solution. The introduction of decay reduces the survival probability, as the second term in Eq. (12) reduces with α. Decay also brings about a deviation from a flat probability towards the high energy end. The dotted line gives the probability for the same Δm^2 but a higher value of $\tan^2\theta$ with $\alpha=10^{-11}$ eV^2. We observe that there is a huge drop in the survival probability initially, followed by a sharp increase with energy. A comparison between the different curves shows that inclusion of decay results in the reduction of the survival probability as well as an energy distortion and both these effects increase with the mixing angle θ.

We next perform a χ^2 analysis of the total rates and the day-night spectrum data for nonzero decay. The best fit comes for $\alpha=0$, corresponding to no decay with the Δm^2 and $\tan^2\theta$ as given in Table I. However, nonzero values of α giving finite decay probability also give an acceptable fit. For small values of θ as in the SMA region, the fraction of ν_2 in the solar neutrino beam is very small. As a result very few neutrinos decay and all values of α may be allowed. On the other hand, in the LMA region the θ is high and a large number of neutrinos can decay, producing a distortion in the energy spectrum. Therefore the data can put some restrictions on the allowed values of α. In Fig. 4 we plot $\Delta\chi^2$ $(=\chi^2-\chi^2_{min})$ vs α keeping the other two parameters free (in the LMA regime). We also show the 99% C.L. limit for three parameters by the dotted line. From Fig. 4 we see that in the LMA region, values of α up to 3.5×10^{-11} eV^2 are allowed at 99% C.L. from the global analysis.

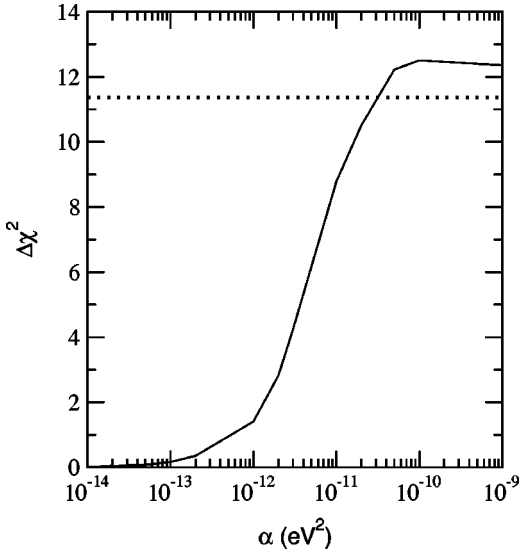

FIG. 4. The $\Delta\chi^2$ versus decay constant α for the global analysis of total rates and the SK day and night spectrum data. Also shown by the dotted line is the 99% C.L. limit for three parameters.

In Fig. 5 we show the allowed regions in the Δm^2 -$\tan^2\theta$ plane for various fixed values of α. The first panel is for $\alpha=0$ which is the case of no decay and the contours are the same as those presented in Fig. 1, modulo the difference in the definition of the C.L. as now there are three parameters whereas in Fig. 1 we had two. The other three panels are for different nonzero allowed values of α obtained from Fig. 4.

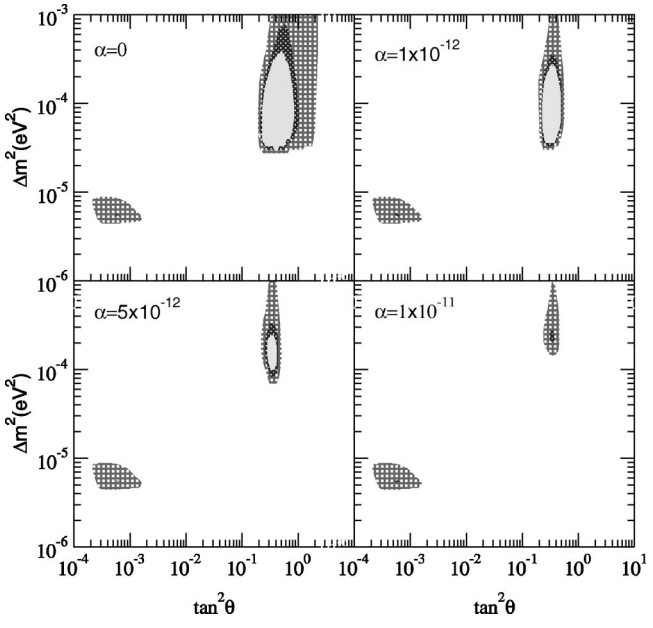

FIG. 5. The 90%, 95%, and 99% C.L. allowed area from the global analysis of the total rates and the 1117-day SK day-night spectrum data, for MSW conversion of unstable neutrinos at various values of the decay constant α. The different fixed values of α in eV^2 are indicated.

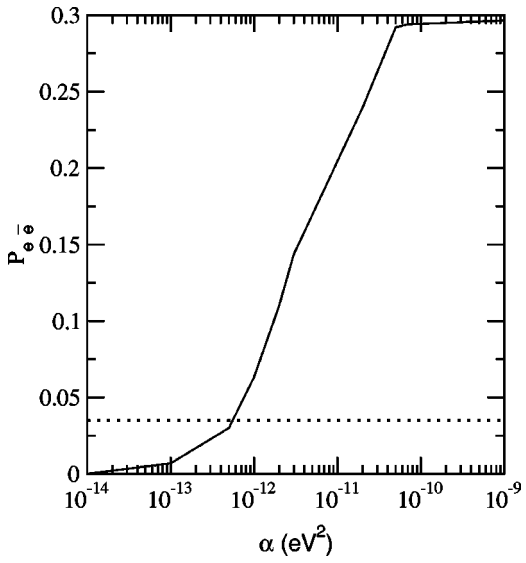

FIG. 6. The conversion probability of ν_e to $\bar{\nu}_e$, P_{ee}^{-} versus decay constant α. Also shown by the dotted line is the 99% C.L. value of P_{ee}^{-} allowed from the nonobservance of $(\bar{\nu}_e - p)$ events in the SK detector.

As expected, we find that the SMA allowed regions remain mostly unaffected due to a nonzero α. The LMA solution on the other hand is appreciably affected and the allowed area shrinks as α increases. This effect is seen to be more pronounced for larger $\tan^2\theta$. The reason for this can be traced down to the fact that decay results in distortion of the high energy end of the neutrino spectrum and this distortion is more for higher $\tan^2\theta$, a feature explicit in Fig. 3. As a result higher values of $\tan^2\theta$ are disfavored by the global data as α increases.

It is to be noted that although in the LOW region the $\sin^2\theta$ is high, the Δm^2 is small and appreciable decay over the Sun-Earth distance is not obtained if one has to be consistent with the bounds on the coupling constant from K decays. Because of this, the LOW region is not plotted in Fig. 5.

The results presented in this section are in general valid for both decay models though in model 2 the ν_2 decays to a $\bar{\nu}_1$, which can interact with the electrons in the SK detector as $\bar{\nu}_e$ and $\bar{\nu}_x$. But since the $\bar{\nu}_1$ is degraded in energy [7], the effect of these additional $(\bar{\nu}_e - e)$ and $(\bar{\nu}_x - e)$ scattering events in SK is not significant [14] and the final results remain the same. However, additional constraints on model 2 come from the $\bar{\nu}_e p \to e^+ n$ events, which contribute to the background in SK. From the absence of a significant contribution above the background, the bound obtained on the total flux of $\bar{\nu}_e$ from ^{8}B neutrinos is $\Phi_{\bar{\nu}_e}(^8\mathrm{B}) < 1.8 \times 10^5$ cm^{-2} s^{-1} which translates to a bound on the probability $P_{ee}^{-} < 3.5\%$ [24]. In Fig. 6 we plot the conversion probability P_{ee}^{-} vs α. For each α we find the χ^2_{min} and plot P_{ee}^{-} for the corresponding the best fit Δm^2 and $\tan^2\theta$. We also show the allowed limit of $P_{ee}^{-} = 0.035$. So from this constraint for model 2 only $\alpha \leqslant 5.8 \times 10^{-13}$ eV^2 remain allowed.

IV. IMPLICATIONS FOR SNO

The main detection processes in the heavy water of SNO are

$$\nu_e + d \to p + p + e^-, \tag{15}$$

$$\nu_x + d \to p + n + \nu_x . \tag{16}$$

The first is a charged current (CC) reaction with energy threshold of 1.44 MeV and the second one is a neutral current (NC) process with an energy threshold of 2.23 MeV. While the CC is sensitive to only ν_e, the NC process is sensitive to neutrinos and antineutrinos of all flavors. The rate of $(\nu_e - d)$ CC events recorded in the detector is given by

$$R_{CC} = \frac{\int dE_\nu \lambda_{\nu_e}(E_\nu)\sigma_{CC}(E_\nu)\langle P_{ee}\rangle}{\int dE_\nu \lambda_{\nu_e}(E_\nu)\sigma_{CC}(E_\nu)}, \tag{17}$$

$$\sigma_{CC} = \int_{E_{A_{th}}} dE_A \int_0^\infty dE_T R(E_A, E_T) \int dE_\nu \frac{d\sigma_{\nu_e d}(E_T, E_\nu)}{dE_T}, \tag{18}$$

where λ_{ν_e} is the normalized ^{8}B neutrino spectrum, $\langle P_{ee}\rangle$ is the time averaged ν_e survival probability, $\mathrm{d}\sigma_{\nu_e d}/\mathrm{dE}_T$ is the differential cross section of the $(\nu_e - d)$ interaction [25], E_T is the true and E_A the apparent (measured) kinetic energy of the recoil electrons, $E_{A_{th}}$ is the detector threshold energy which we take as 5 MeV, and $R(E_A, E_T)$ is the energy resolution function which is assumed to be Gaussian:

$$R(E_A, E_T) = \frac{1}{\sqrt{2\pi}(0.348\sqrt{E_T/\mathrm{MeV}})} \times \exp\left(- \frac{(E_T - E_A)^2}{0.242 E_T \ \mathrm{MeV}} \right). \tag{19}$$

The NC event rate is given by

$$R_{NC} = \frac{\int dE_\nu \lambda_{\nu_e}(E_\nu)\sigma_{NC}(E_\nu)\mathcal{P}}{\int dE_\nu \lambda_{\nu_e}(E_\nu)\sigma_{NC}(E_\nu)}, \tag{20}$$

where $\mathcal{P} = \langle P_{ee}\rangle + \langle P_{e\mu}\rangle$ for two-flavor ν_e-ν_μ oscillations. The left hand panels in Fig. 7 give the range of predicted values of R_{CC}, R_{NC}, and the double ratio R_{NC}/R_{CC} at 99% C.L. from a global MSW analysis of the solar neutrino data. The black dots in these figures represent the expected rates in SNO for the local best-fit values of the parameters obtained. As the neutral current interaction is flavor blind, the R_{NC} remains 1 for oscillations to active neutrinos for which $\mathcal{P} = 1$. But for oscillations to sterile neutrinos $\mathcal{P} = \langle P_{ee}\rangle$ and $R_{NC} = 0.78$ for the best-fit case.

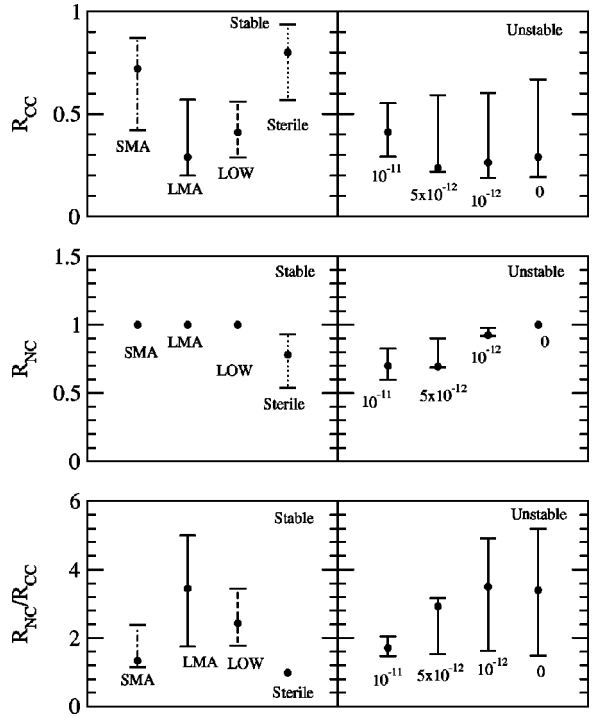

FIG. 7. The predicted ranges of R_{CC}, R_{NC} and R_{NC}/R_{CC} in SNO for the standard MSW conversion to stable neutrinos (left hand panels) and for unstable neutrinos (right hand panels). The dots give the values of the rates for the local best fit.

The right hand panels in Fig. 7 show the corresponding rates in SNO for the LMA region if the neutrinos are assumed to be unstable (the SMA solution remains largely unaffected as discussed in the previous section). We consider the decay model 1 and present the 99% C.L. predicted range of values of the rates for three different allowed values of the parameter α, along with the case for $\alpha=0$, which is the same as the LMA region of the global MSW analysis, modulo the difference in the definition of the C.L. Also shown are the rates for the best-fit value of Δm^2 and $\tan^2\theta$ for various fixed values of α. For each fixed value of Δm^2 and $\tan^2\theta$ one expects R_{CC} to fall sharply with α. But since the best fit of the global analysis for increasing α corresponds in general to a higher Δm^2, that raises the value of R_{CC}. Hence R_{CC} in SNO alone may not be able to distinguish the decay scenario from MSW conversion to active stable neutrinos. The value of R_{NC} suffers a marked decrease from 1 as the decay constant α increases, since for the decay model 1 the ν_e decays to sterile particles which cannot be detected in SNO.

From Fig. 7 we see that if R_{NC} is below 1, one can have either MSW conversion to sterile neutrinos or the possibility of unstable neutrinos. But the ambiguity between the last two cases can be lifted if one next looks at the value of R_{CC}, which is much lower for the case of unstable neutrinos than what one would get for MSW conversion to sterile neutrinos. We also display the expected range of R_{NC}/R_{CC} for various fixed values of the decay constant. It is clear from the figure that from the value of R_{NC}/R_{CC} in SNO one can clearly distinguish the case of a decay from the case of a MSW transition to sterile neutrinos.

In the decay model 2 the ν_e decay to $\bar{\nu}_1$, which can in principle show up both in the NC events in SNO as well as in the charged current absorption reaction

$$\bar{\nu}_e + d \rightarrow n + n + e^+. \tag{21}$$

But since the absence of $(\bar{\nu}_e - p)$ events in SK restrict $\alpha \leqslant 5.8\times10^{-13}$ eV^2, both the additional contribution to the NC event and the $(\bar{\nu}_e - d)$ absorption is negligible in SNO.

V. CONCLUSIONS

We have investigated the effect of neutrino decay on the MSW solution to the solar neutrino problem. There are two factors which control the effect of decay: (i) the mixing angle θ which determines the fraction of the unstable component in the ν_e beam; (ii) the decay constant α which determines the decay rate.

In order for the neutrinos to decay over the Earth-Sun distance α should be $\geqslant 10^{-13}$ eV^2. Then Eq. (2) and the bounds on the coupling constant from K decays restrict $\Delta m^2 \gtrsim 10^{-7}$ eV^2 and decay does not take place in the LOW region. We therefore probe the SMA and the LMA regions. We find that even the SMA region is not affected much because the mixing angle being small very few neutrinos would decay. But the effect of decay on the LMA region is significant. This is borne out by the χ^2 analysis of the global solar data on rates and SK day-night spectrum. We point out that although the data *prefer* no decay, it still *cannot rule out* the possibility of unstable neutrinos completely. We put limits on the allowed range of the decay constant α and present the allowed areas in the Δm^2-$\tan^2\theta$ parameter space for various allowed values of α. The LMA allowed zone is seen to be severely constrained by decay.

From Fig. 4, values of $\alpha \leqslant 3.5\times10^{-11}$ eV^2 are allowed, implying a neutrino rest frame lifetime $\tau_0 \geqslant 2\times10^{-5}$ sec. Thus one may encounter decay before neutrino decoupling in the early universe. This may result in increasing the number of light neutrinos, N_ν, to greater than 3. However, the upper limit on N_ν can be as large as 6 [26]. Hence our decay model is consistent with the bounds from the early universe.

From the fact that the neutrinos from SN1987A have not decayed on their way one gets a lower bound on the electron neutrino lifetime as $\tau > 5.7\times10^5 (m_{\nu_e}/\text{eV})$ sec. However, if one includes neutrino mixing, then shorter lifetimes are allowed provided $|U_{e2}| < 0.9$ [27]. This again is consistent with our analysis.

In this paper we assume one of the neutrino states to be unstable in vacuum and the values of the decay constant α are such that one has decay over the Earth-Sun distance. For these values of α, decay inside the Sun or the Earth is negligible. However, as was shown in [28] matter can induce neutrino decay with Majoron emission even when neutrinos are stable in vacuum. It was shown later in [29] that in the presence of only standard interactions, matter induced decay cannot provide a solution to the solar neutrino problem due to the strong bounds on neutrino-Majoron couplings. As we have discussed in this paper, decay models where the ν_2

decays to a $\overline{\nu}_1$ and a Majoron are independently disfavored from the nonobservation of $(\overline{\nu}_e - p)$ events in SK.

We have looked at the implications of unstable neutrinos for the SNO detector. We first present the values of the CC and NC rates which SNO is expected to observe for MSW transitions with stable neutrinos. We have given the values for transitions to both active as well as sterile species. For unstable neutrinos the NC rate is less than 1 and comparable to R_{NC} for standard MSW SMA transitions to sterile neutrinos. But even though the value of R_{NC} may be nearly the same for the two scenarios, comparing the values of R_{CC} or R_{NC}/R_{CC} it may be possible in principle to distinguish the decay scenario from the MSW transition to sterile neutrinos.

ACKNOWLEDGMENTS

The authors wish to thank Carlos Peña-Garay for many useful discussions during the development of the solar code, Y. Suzuki for sending them the SK data, and H.M. Antia for many helpful discussions.

[1] B. T Cleveland *et al.*, Nucl. Phys. B (Proc. Suppl.) **38**, 47 (1995); Kamiokande Collaboration, Y. Fukuda *et al.*, Phys. Rev. Lett. **77**, 1683 (1996); GALLEX Collaboration, W. Hampel *et al.*, Phys. Lett. B **388**, 384 (1996); SAGE Collaboration, J. N. Abdurashitov *et al.*, Phys. Rev. Lett. **77**, 4708 (1996); GNO Collaboration, M. Altmann *et al.*, Phys. Lett. B **490**, 16 (2000).

[2] The results presented at the nu2000 meeting at Sudbury, Canada, 2000, can be found at http://nu2000.sno.laurentian.ca

[3] M. C. Gonzalez-Garcia and C. Peña-Garay, Nucl. Phys. B (Proc. Suppl.) **91**, 80 (2000).

[4] O. G. Miranda, C. Peña-Garay, T. I. Rashba, V. B. Semikoz, and J. W. F. Valle, Nucl. Phys. **B595**, 360 (2001); D. Majumdar, A. Raychaudhuri, and A. Sil, Phys. Rev. D **63**, 073014 (2001); A. M. Gago, H. Nunokawa, and R. Zukanovich Funchal, hep-ph/0012168; M. M. Guzzo, H. Nunokawa, P. C. de Holanda, and O. L. G. Peres, hep-ph/0012089.

[5] R. S. Ragahavan, X. He, and S. Pakvasa, Phys. Rev. D **38**, 1317 (1988).

[6] M. Fukugita, Phys. Rev. D **36**, 3817 (1987).

[7] A. Acker, S. Pakvasa, and J. Pantaleone, Phys. Rev. D **43**, R1754 (1991); **45**, R1 (1992).

[8] A. Acker, A. Joshipura, and S. Pakvasa, Phys. Lett. B **285**, 371 (1992).

[9] G. B. Gelmini and M. Roncadelli, Phys. Lett. **99B**, 411 (1981).

[10] LEPEWG report, http://www.cern.ch

[11] A. Acker and S. Pakvasa, Phys. Lett. B **320**, 320 (1994).

[12] V. Barger, W. Y. Keung, and S. Pakvasa, Phys. Rev. D **25**, 907 (1982).

[13] D. O. Caldwell *et al.*, Phys. Rev. Lett. **59**, 419 (1987); P. Fisher *et al.*, Phys. Lett. B **192**, 460 (1987).

[14] S. Choubey, S. Goswami, and D. Majumdar, Phys. Lett. B **484**, 73 (2000).

[15] L. Wolfenstein, Phys. Rev. D **34**, 897 (1986); S. P. Mikheyev and A. Yu. Smirnov, Yad. Fiz. **42**, 1441 (1985) [Sov. J. Nucl. Phys. **42**, 913 (1985)]; Nuovo Cimento **9**, 17 (1986).

[16] S. T. Petcov, Phys. Lett. B **200**, 373 (1988).

[17] A. S. Dighe, Q. Y. Liu, and A. Yu. Smirnov, hep-ph/9903329 and references therein.

[18] SK Collaboration, Y. Suzuki (private communication).

[19] S. Goswami, D. Majumdar, and A. Raychaudhuri, Phys. Rev. D **63**, 013003 (2001).

[20] J. N. Bahcall, S. Basu, and M. Pinsonneault, astro-ph/0010346.

[21] G. L. Fogli and E. Lisi, Astropart. Phys. **3**, 185 (1995).

[22] M. C. Gonzalez-Garcia and C. Peña-Garay, Phys. Rev. D **63**, 073013 (2001).

[23] M. C. Gonzalez-Garcia, P. C. de Holanda, C. Peña-Garay, and J. W. F. Valle, Nucl. Phys. **B573**, 3 (2000).

[24] P. Vogel and J. F. Beacom, Phys. Rev. D **60**, 053003 (1999); E. Torrente-Lujan, Phys. Lett. B **494**, 255 (2000).

[25] S. Nakamura, T. Sato, V. Gudkov, and K. Kubodera, Phys. Rev. C **63**, 034617 (2001).

[26] K. Olive and D. Thomas, Astropart. Phys. **11**, 403 (1999); E. Lisi, S. Sarkar, and F. Villante, Phys. Rev. D **59**, 123520 (1999); S. Burles, K. Nollett, J. Truran, and M. S. Turner, Phys. Rev. Lett. **82**, 4176 (1999).

[27] J. Frieman, H. Haber, and K. Freese, Phys. Lett. B **200**, 115 (1988).

[28] Z. G. Berezhiani and M. I. Vysotsky, Phys. Lett. B **199**, 281 (1987).

[29] Z. G. Berezhiani and A. Rossi, hep-ph/9306278.